Coulomb-nuclear interference with deuterons: Isospin character of the 2_1^+ and 3_1^- excitations in ^{94,98}Mo

G. M. Ukita,[1,2] T. Borello-Lewin,[1] L. B. Horodynski-Matsushigue,[1] J. L. M. Duarte,[1] and L. C. Gomes[1]
[1]*Instituto de Física, Universidade de São Paulo, C.P. 66318, 05315-970 São Paulo, SP, Brazil*
[2]*Faculdade de Psicologia, Universidade de Santo Amaro, Rua Professor Enéas de Siqueira Neto, 340, 04829-300 São Paulo, SP, Brazil*
(Received 27 November 2000; published 19 June 2001)

Angular distributions of inelastic-scattering cross sections were measured for deuterons of 13.2 and 16.0 MeV, exciting the 2_1^+ and 3_1^- states of ^{94}Mo and ^{98}Mo. The analysis of the Coulomb-nuclear interference patterns displayed by these angular distributions was favored by the quality of the data obtained with the S. Paulo Pelletron-Enge-Spectrograph facility. The distorted-wave Born approximation–deformed-optical-model analysis with global parameters yielded values for the ratio $C_L = \delta_L^C / \delta_L^N$ and for δ_L^N (where δ_L^C and δ_L^N are, respectively, the charge and isoscalar deformation lengths), which inform the reader about the isospin character of the excitations. A reduced isoscalar transition probability, $B(ISL)$, was defined, in analogy to $B(EL)$, the ratio $B(EL)/B(ISL)$ being proportional to the square of C_L. The latter quantity is, however, experimentally better determined. The results obtained for C_2, C_3, δ_2^N, and δ_3^N at the two incident energies, 13.2 and 16.0 MeV, are consistent for each ^{94}Mo and ^{98}Mo. The values of C_L reveal a slight predominance of the protons in the quadrupolar transitions, in both ^{94}Mo and ^{98}Mo. The 2_1^+ and the 3_1^- states are more collective in ^{98}Mo than in ^{94}Mo, both with respect to the protons (charge) and with respect to protons and neutrons (mass).

DOI: 10.1103/PhysRevC.64.014316 PACS number(s): 21.10.Re, 25.45.De, 27.60.+j

I. INTRODUCTION

The Mo isotopes are of special interest for a comparative study of the collective properties of low-lying excitations, as they are neighbors, just one proton pair above the challenging $_{40}$Zr chain, where extremely rapid modifications occur as neutrons are added to the semimagic ^{90}Zr nucleus or, with still more dramatic consequences, to ^{96}Zr [1,2]. Indeed, if characterized, as usual, by the excitation energy $E_{\rm exc}$ and by the reduced electric transition probability $B(E2)$ to the first quadrupolar excitation, ^{90}Zr behaves almost like a doubly magic nucleus. The neighbors ^{92,94}Zr present intermediate values for these structure characteristics, but in ^{96}Zr, both $Z=40$ and $N=56$, seem well-closed subshells. This pattern is suddenly disrupted and ^{100}Zr presents several features of a well-deformed shape, such as a very low $E_{\rm exc}(2_1^+)$ and a high $B(E2)$. Each isotopic chain in this region, up to $_{46}$Pd, shows some kind of transition around $N=56$ being washed out as Z is increased. The addition of neutrons, above this critical value, seemingly polarizes the proton distribution, enhancing the collectivity, which is taken as prolate deformed for the heavier Zr nuclei [2,3], γ soft, or even triaxial for Ru or Pd [3–5].

The characteristics of the first excited 2^+ states have, for a long time, been extensively used as nuclear structure indicators in comparison between experiment and model expectations, but they are usually inferred through $B(E2)$ values, which, in principle, are related only to the charge contributions to the excitation. Since it is clear that neutrons play, in this part of the nuclear chart, a primordial role in defining the collective behavior, it is important to assess also the reduced isoscalar transition probability $B(IS2)$. This is conveniently done through the study of inelastic scattering of isoscalarly interacting projectiles with incident energies such as to enhance Coulomb-nuclear interference [6], which allows for the simultaneous extraction of $B(ISL)$ and $B(EL)$ values for those excitations for which a predominant multipolarity L can be defined.

This paper presents a study of Coulomb-nuclear interference (CNI) in the inelastic scattering of deuterons on ^{94}Mo, an isotone of ^{92}Zr, and also on ^{98}Mo, which is an isotone of both ^{96}Zr and ^{100}Ru, for which quite different isospin characteristics of the low-lying quadrupolar excitations have been previously verified [7,8]. Coulomb-nuclear interference results have, to our knowledge, not been formerly reported for deuterons, due to experimental difficulties associated with the beam, in spite of this projectile being, in principle, a convenient choice for these studies. In fact, the huge amount of experimental information collected for deuteron reactions contributes to the pinning down of the parameters needed to phenomenologically describe the interaction of this projectile with the nuclei of interest. Therefore, the use of deuterons helps to keep the free parameters in the analysis under control, which is especially important if comparative conclusions, in the study of several isotopic chains, are to be drawn.

In the present work, besides analyzing the transitions to the 2_1^+ states in ^{94,98}Mo, $B(IS3)$ and $B(E3)$ values for the first octupolar excitations could also be extracted, since their angular distributions showed enough of the interference pattern to discriminate a value for their ratio, although with much lower precision.

II. EXPERIMENTAL PROCEDURE

For deuterons of some 10 to 20 MeV on medium mass nuclei, the interference minimum between the Coulomb and nuclear excitations appears at relatively forward angles. Detection techniques employing nuclear emulsions at the focal surface of the Enge spectrograph, in association with the excellent beam profile and energy characteristics provided by the São Paulo Pelletron facility, are, therefore, important

TABLE I. Isotopic composition of the molibdenum targets (Oak Ridge Separated Isotopes Division).

	Abundance (%)						
Target	^{92}Mo	^{94}Mo	^{95}Mo	^{96}Mo	^{97}Mo	^{98}Mo	^{100}Mo
^{94}Mo	0.87	93.90	2.85	1.04	0.40	0.75	0.22
^{98}Mo	0.32	0.22	0.45	0.59	0.69	97.18	0.55

means for obtaining the necessary quality of the data for these CNI studies. Additional care must be applied to the focusing conditions. Current intensity ratios of 1:30 and 1:100, in comparison between slits and beam, were achieved in the present experiment, respectively, on the defining slits before the target (1.0×2.0 mm^2) and on a circular slit of $\phi\sim6$ mm (situated approximately half a meter upstream). The deuteron beams of 13.2 MeV, or alternatively 16.0 MeV, impinged on uniform and thin (~30 μg/cm^2) enriched targets of ^{94}Mo or ^{98}Mo. Targets were made by a well-controlled electron bombardment evaporation technique [9] of metallic Mo (^{94}Mo targets) and MoO_3 (^{98}Mo targets), both in powder form, onto thin carbon backings (~10 μg/cm^2). Table I presents the isotopic composition of the material employed in the fabrication of the targets. The scattered deuterons were momentum analyzed by the S. Paulo Enge split-pole spectrograph and detected in nuclear emulsion (in the present study, Ilford G5 or equivalent, 50 μm thick). Aluminum foils, thick enough to absorb heavier reaction products, covered the emulsion. The use of nuclear emulsion enormously reduces the background associated with deuteron beams, since these detectors do not respond to the abundant neutron, γ, and x ray radiations that are produced, in particular, in the presence of the iron core of the spectrograph. In fact, the background observed in the spectra is mostly due to the tail of the elastic peak and is therefore extremely dependent on beam focusing.

In the present work, inelastic-scattering spectra were measured, for both isotopes, at 18 scattering angles from $\theta_{lab}=12.5°$ to 80° for the incident energy of 13.2 MeV and at eight angles between $\theta_{lab}=14°$ and 76° for 16.0 MeV. The solid angle of admittance to the spectrograph was maintained fixed, corresponding to $\Delta\theta_{lab}=\pm1.9°$. The emulsion plates were scanned, after processing, in strips of 200 μm across the plates and energy resolutions of ~8 and ~12 keV, full width at half maximum (FWHM), were achieved, respectively, in the spectra corresponding to 13.2 and 16.0 MeV incident energies.

Typical examples of the complete spectra of inelastic deuteron scattering obtained with the emulsion technique, on ^{94}Mo at $\theta_{lab}=58°$ and on ^{98}Mo at $\theta_{lab}=60°$, both for the incident energy of 13.2 MeV, are presented in Fig. 1. To illustrate the quality of the data, Fig. 2 shows part of four further spectra, displaying the peak associated with the first quadrupolar excitation in ^{98}Mo at 13.2 and 16.0 MeV incident energies. Figure 3, in a similar way, shows examples of the relevant part of the spectra for the octupolar excitation, observed for the same isotope at 16.0 MeV. As put into evidence by the spectra at forward angles, the good energy resolution of ~8 keV is essential to enhance the peak with respect to the background. This background, mainly associated with the elastic tail, drops with increasing scattering angle, as can be seen in the spectra at $\theta_{lab}=16°$ and $\theta_{lab}=26°$ [Figs. 2(a) and 2(b)]. Figure 2(d) also illustrates the judicious choice of the scattering angles, made to avoid that the peak of interest be hidden by the broad peaks associated with the presence of known contaminants in the target (which are, in general, not focused).

For the relative normalization of the spectra, the total number of incident deuterons was determined by a current integrator, which measured the charge collected in a Faraday cup (with electron suppression), while the direction of the beam was continuously monitored. Absolute normalization of the cross sections was referred to optical-model predictions for elastic-scattering of deuterons on the same target,

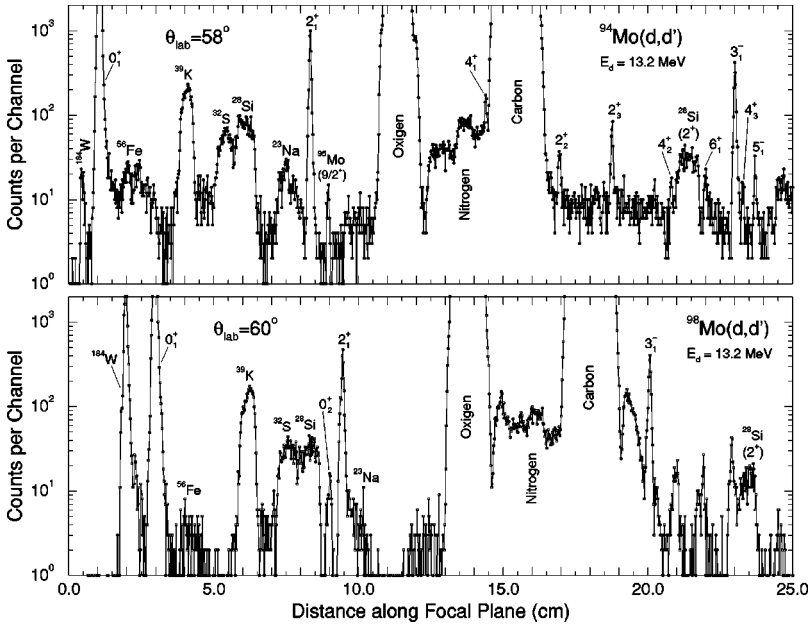

FIG. 1. Examples of spectra of ^{94}Mo(d,d') and ^{98}Mo(d,d') at 13.2 MeV, taken, respectively, at $\theta_{lab}=58°$ and $\theta_{lab}=60°$.

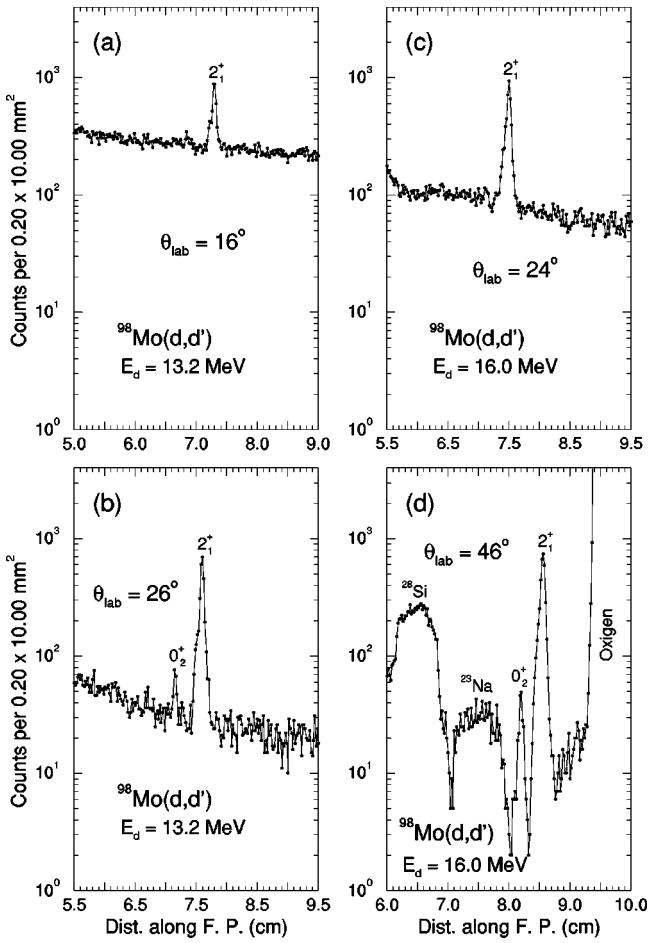

FIG. 2. Portions of the spectra of ^{98}Mo(d,d') for the 2_1^+ state, taken at 13.2 MeV, for (a) $\theta_{lab}=16°$ and (b) $\theta_{lab}=26°$, and at 16.0 MeV, for (c) $\theta_{lab}=24°$ and (d) $\theta_{lab}=46°$. Observe the very compressed log scale for the *y* coordinate.

measured under similar conditions. Figure 4 displays the elastic-scattering angular distributions for ^{94,98}Mo, measured at 13.2 and 16.0 MeV, in comparison with the optical-model predictions. The parameters of the systematics of Perey and Perey for deuterons [10] are employed in the normalization (see Table II). A maximum scale change of $\sim 3\%$ would be produced if the global optical-model predictions of Daehnick *et al.* [11], were taken. Due, furthermore, to target nonuniformity, plate scanning, and statistics in the elastic data, a maximum uncertainty of $\sim \pm 5\%$, for 13.2 MeV incident energy measurements, and $\sim \pm 7\%$, for 16.0 MeV, is estimated in the absolute cross section scale, for both isotopes.

III. ANALYSIS

Due to the relatively high excitation energies of the 2_1^+ states (871 keV for ^{94}Mo and 787 keV for ^{98}Mo) and not so high values of the deformation lengths, no appreciable coupling between ground and excited states has to be taken into acount in the reaction analysis. Thus, the well-established distorted-wave Born approximation (DWBA) could be employed. Incomplete information on the relevant aspects of the nuclear structure, beside the well-known difficulty to describe microscopically the imaginary part of the potential [12], point to the use of a macroscopic description of the excitation, in terms of what is usually called a deformed optical-model potential (DOMP), since the priority is on a comparative analysis throughout the region.

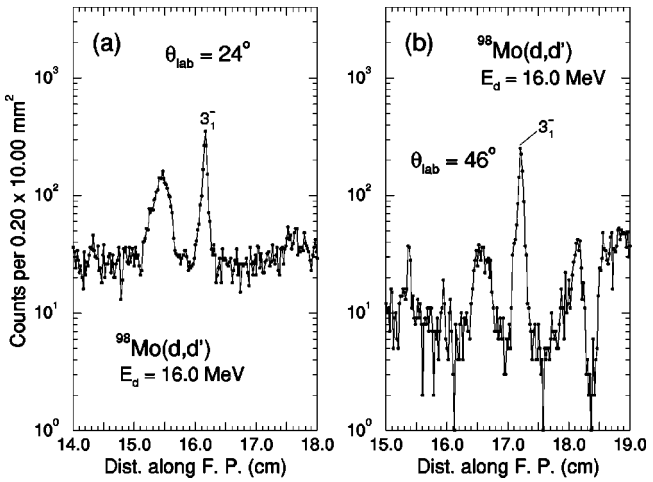

FIG. 3. Portions of the spectra of ^{98}Mo(d,d') for the 3_1^- state, taken at 16.0 MeV, for (a) $\theta_{lab}=24°$ and (b) $\theta_{lab}=46°$. Observe the very compressed log scale for the *y* coordinate.

In the DWBA-DOMP approach, the same phenomenological optical model describes both, the distorted waves in incident and exit channels and the transition potential to the collective state. The intensity of the excitation characterized by the deformation length extracted [12].

The DWBA-DOMP angular distributions were calculated by means of the code DWUCK4 [13], considering the influence of Coulomb excitation up to distances of 80 fm from the nuclear center. The macroscopic collective form factors [12], responsible, respectively, for the nuclear $F_L^N(r)$, and Coulomb $F_L^C(r)$ excitation processes, were taken as

$$F_L^N(r) = -\delta_{R,L}^N(U)\frac{dV(r)}{dr} - i\,\delta_{I,L}^N(U)\frac{dW_D(r)}{dr}, \qquad (1)$$

where V and W_D are the real and surface imaginary depths of the optical potential U, with the standard Woods-Saxon and derivative Woods-Saxon dependencies, with given geometrical parameters (r_R, a_R and r_I, a_I), and

$$F_L^C(r) = \begin{cases} \dfrac{4\pi Z_a e}{2L+1}[B(EL)]^{1/2}\dfrac{1}{r^{L+1}}, & \text{for } r \geqslant R_c \\ 0, & \text{for } r < R_c, \end{cases}$$

where $R_c = r_c A^{1/3}$ is the characteristic radius of the charge distribution. To take the Coulomb form factor as zero inside the charge distribution does not affect the results, since for the deuteron energies considered in this work, the reaction proceeds peripherically.

A charge deformation length $\delta_L^C = \beta_L^C R_c$, where β_L^C is the known deformation parameter [1], may be defined

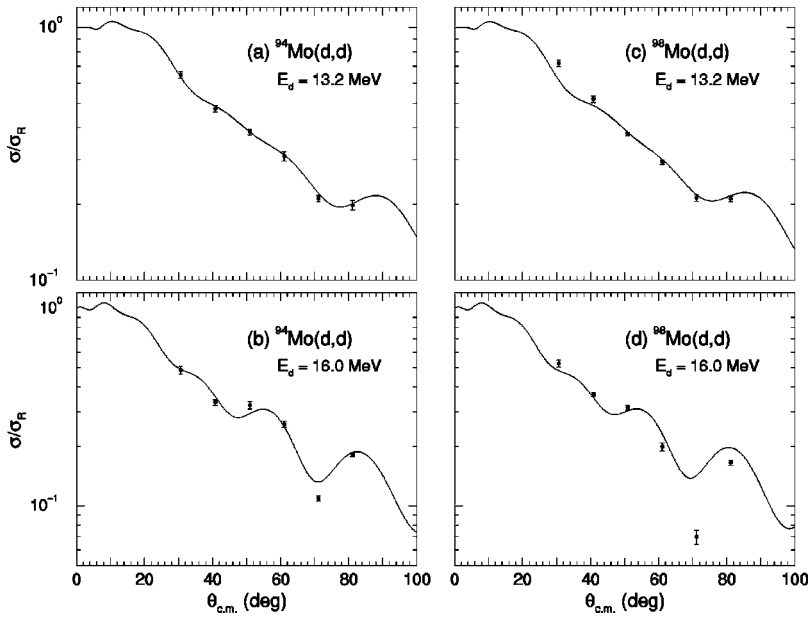

FIG. 4. Angular distributions for the elastic scattering of deuterons, in comparison with optical-model predictions [10]: (a) ^{94}Mo(d,d) at 13.2 MeV, (b) ^{94}Mo(d,d) at 16.0 MeV, (c) ^{98}Mo(d,d) at 13.2 MeV, and (d) ^{98}Mo(d,d) at 16.0 MeV.

$$\delta_L^C = \left(\frac{4\pi}{3ZR_c^{L-1}}\right)\frac{[B(EL)]^{1/2}}{e}. \tag{2}$$

The isoscalar deformation length $\delta_{R,L}^N(U) = \delta_{I,L}^N(U) = \delta_L^N$ may similarly be related to $B(ISL)$, through the following expression:

$$B(ISL) = (\delta_L^N)^2\left[\frac{3ZR_m^{L-1}}{4\pi}\right]^2, \tag{3}$$

where $R_m = r_m A^{1/3}$ is the characteristic radius of the mass distribution. Normalization to Z is preferred to the normalization to A employed by some authors [14].

For convenience of analysis, the parameters δ_L^N and $C_L = \delta_L^C/\delta_L^N$ were chosen to describe the collective excitations. Thus,

$$\frac{B(EL)}{B(ISL)} = e^2\left(\frac{\delta_L^C}{\delta_L^N}\right)^2\left[\frac{R_c^{L-1}}{R_m^{L-1}}\right]^2 = e^2 C_L^2\left(\frac{r_c}{r_m}\right)^{2L-2}. \tag{4}$$

TABLE II. Global optical-model parameters for elastic deuteron scattering prescribed by Perey and Perey [10]. A Coulomb reduced radius of $r_c = 1.22$ fm was utilized.

A	E_d (MeV)	V (MeV)	r_R (fm)	a_R (fm)	W_D (MeV)	r_I (fm)	a_I (fm)
94	13.2	96.6	1.15	0.81	17.6	1.34	0.68
98	13.2	96.3	1.15	0.81	17.6	1.34	0.68
94	16.0	96.0	1.15	0.81	18.3	1.34	0.68
98	16.0	95.7	1.15	0.81	18.3	1.34	0.68

It is, therefore, seen that the parameter C_L contains the relevant information about the ratio of the charge (protons) with respect to the mass (protons + neutrons) contributions to the excitation of the particular state under observation. Grossly speaking, a value of $C_L = 1.0$ characterizes an excitation for which $B(EL)/e^2$ is, within the definition adopted, numerically equal to $B(ISL)$, implying that protons and neutrons contribute to it in the ratio of Z/N, that is an excitation usually referred to as being of homogeneous collective nature.

In the analysis, the distorted waves play an important role in defining the structures of the angular distributions. To make significant comparisons of CNI results, it is, therefore, convenient to maintain the optical-model parameters within a globally established systematics, as far as allowed by the data. The Perey and Perey [10] parameters (see Table II) have the best experimental basis in this deuteron energy region and have been adopted.

Inspection of Fig. 5, where DWBA-DOMP predictions are displayed for three values of incident deuteron energies, demonstrates the discriminative power of the CNI method, in the mass region of interest. The predicted angular distributions were calculated with global optical parameters taken from the systematics of Perey and Perey [10], for typical values of C_2 and δ_2^N, taking the ^{94}Mo($0_1^+ \rightarrow 2_1^+$) excitation as an example. It may be seen that an interference minimum develops for all incident energies: at $\theta_{\text{c.m.}} \sim 30°$ for $E_d = 10.0$ MeV and $\theta_{\text{c.m.}} \sim 15°$ for $E_d = 16.0$ MeV. On the other hand, the typical ''diffractive'' oscillations, due to the nuclear excitation, practically determine the shape of the angular distribution for the more backward angles. Therefore, good data around the interference minimum are essential for the extraction of C_2, while the larger angle data mostly give the global normalization constant $(\delta_2^N)^2$. At $E_d = 10.0$ MeV, discrimination of C_2 in the interval $0.8 \leqslant C_2 \leqslant 1.2$ depends on the possibility of taking data with very small statistical errors in the angular region $25° \leqslant \theta_{\text{c.m.}} \leqslant 35°$. It is clear that the incident energy region of about 13

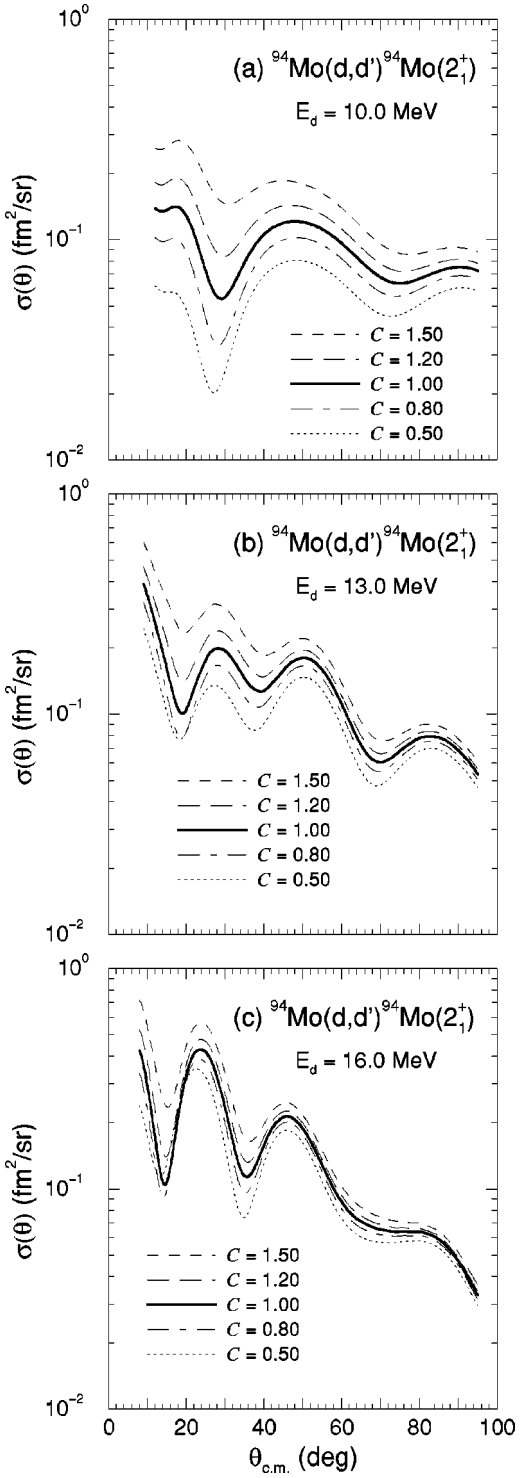

FIG. 5. DWBA-DOMP predictions for the quadrupolar excitation of ^{94}Mo(d,d'), for three incident deuteron energies and several values of $C=C_2=\delta_2^C/\delta_2^N$. A typical value of $\delta_2^N=0.8$ fm was employed.

MeV presents the best discrimination for the parameters of interest. In fact, it is for this incident energy region that the value of C_2, besides the minimum, also substantially affects the ratio of the heights of the two subsequent maxima of the angular distribution. The nonlinearity of the predictions as function of C_2 is also evident at $E_d=16.0$ MeV, with attention being called especially to the shape of the curves for the outmost values of $C_2=0.5$ and $C_2=1.5$, the former ones crossing those for $C_2=0.8$–1.2 near the interference minimum, rendering discrimination of C_2 much more difficult than at 13 MeV. To examine the consistency of the values extracted for the parameters of interest, it was decided to take detailed data at 13.2 MeV and complementary ones at 16.0 MeV.

If the relations

$$B(ISL)=\left|\frac{Z}{A}(\mathbf{M_n}+\mathbf{M_p})\right|^2 \tag{5}$$

and

$$B(EL)=e^2|\mathbf{M_p}|^2, \tag{6}$$

consistent with the here adopted definition of $B(ISL)$, are employed, the assumption of proportionality of neutron and proton transition densities leads to the following equation for the multipolar moments of the neutron and proton distributions:

$$\frac{M_n}{M_p}=\left|\frac{\mathbf{M_n}}{\mathbf{M_p}}\right|=\frac{A}{Z}\left|\frac{B(ISL)}{B(EL)/e^2}\right|^{1/2}-1=\frac{A}{Z}\left(\frac{r_m}{r_c}\right)^{L-1}C_L^{-1}-1. \tag{7}$$

The experimentally well-determined parameter C_L informs, thus, about the isospin character of the excitation with multipolarity L.

A. Quadrupolar excitations

As previously discussed, the characterization of the CNI for the quadrupolar excitations is favored at the lower energy of 13.2 MeV, while the data at 16.0 MeV are mostly employed to check the consistency of the δ^N results. The DWBA-DOMP predictions, with global optical potential parameters, were fitted to the data [6] through the Gauss-Marquardt procedure, searching simultaneously on the values of three parameters, C_2, δ_2^N (13.2 MeV), and δ_2^N (16.0 MeV), which result in a minimum for χ^2. Thus, data at both energies were considered in the fit, constraining for the same value of C_2. The resulting fits to the angular distributions associated with the first 2^+ excitation in ^{94,98}Mo, at 13.2 and 16.0 MeV incident deuteron energies, are shown in Fig. 6. Solid lines refer to the results obtained if r_R and r_I are increased by 2% above the values of Table II. Also shown, as dashed lines, are the fits corresponding to the unmodified global parameters. The reduction of about a factor of 2 in the minimum χ^2 values of the simultaneous fit of the angular distributions, at the two incident energies for both isotopes, points possibly to a physical significance of the increased radii. In the inelastic scattering of deuterons, those nuclei seem, thus, to be represented by a somewhat larger object than in elastic scattering. The rather good stability of the resulting values (with and without the modification of the radii) for δ_2^N and C_2, for both isotopes, as may be appreci-

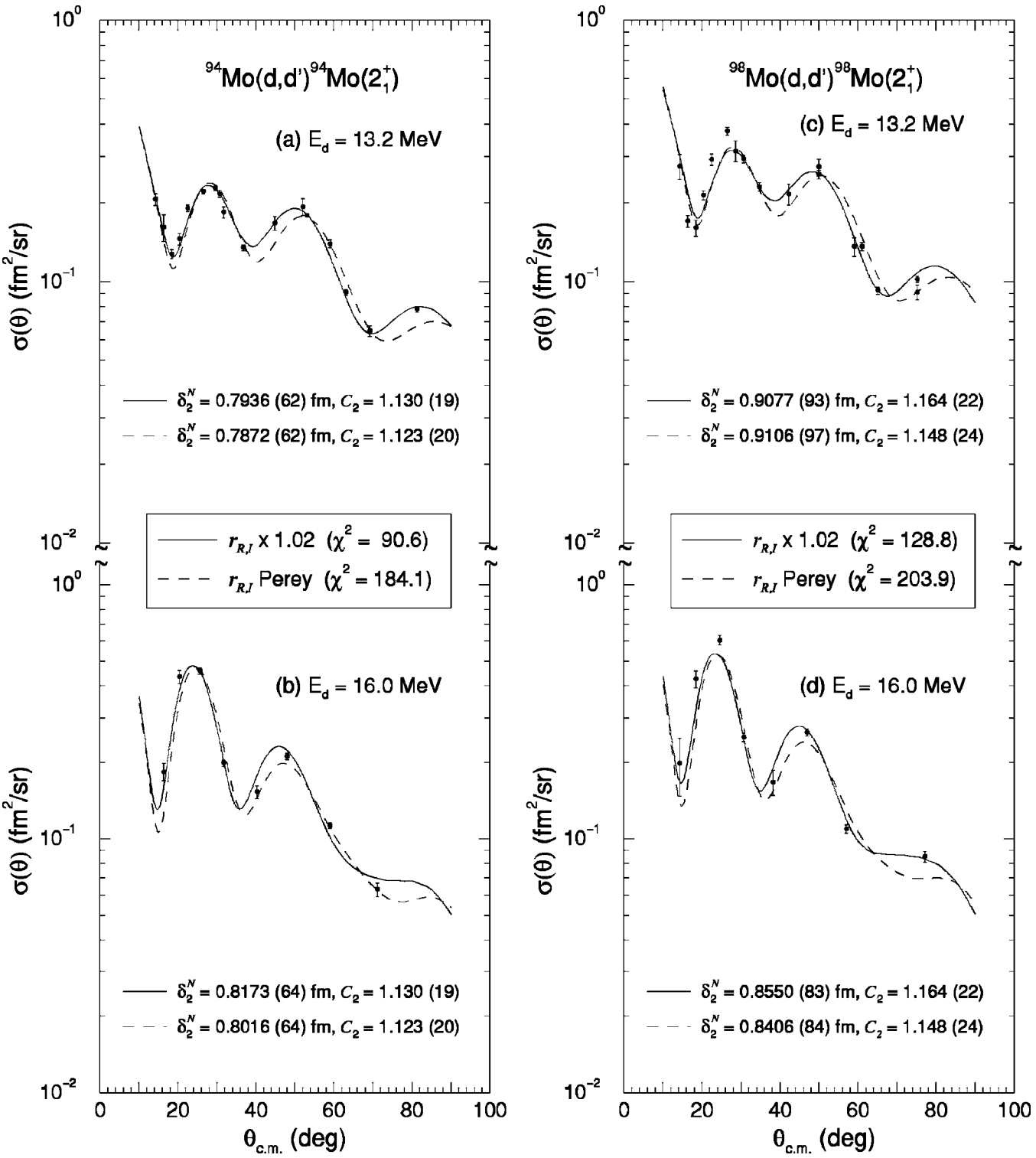

FIG. 6. Experimental angular distributions for the quadrupolar excitations in ^{94}Mo and ^{98}Mo, at two incident deuteron energies, in comparison with DWBA-DOMP best fits, for which the same value of C_2 was imposed. Solid lines correspond to the predictions for increased radii (+2%), while broken lines correspond to the predictions with the original Perey-Perey parameters. The χ^2 values characterize the quality of the constrained simultaneous fit to both angular distributions, for each isotope.

ated by comparing the values in the captions of Fig. 6, supports the confidence in the method of analysis employed here.

It is seen that for ^{94}Mo, the fit of the DWBA-DOMP predictions to the data reproduces the experimental shape very well, if the 2% increase of the real and imaginary radii is applied to the global optical parameters. On the other hand, the angular distributions for ^{98}Mo are, at both energies, somewhat more structured at the first maximum displayed than is predicted by the interpretation at hand. No possible

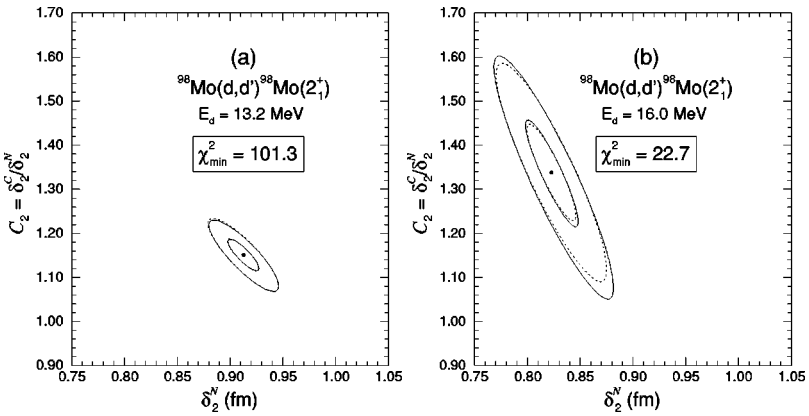

FIG. 7. Comparison of the contour lines for constant χ^2 (solid lines) with the ellipses, which result from the Gauss-Marquardt method (broken lines) for intervals corresponding to, respectively, 68.3% ($\Delta\chi^2=2.3$) and 99.7% ($\Delta\chi^2=11.8$), of statistical confidence, in the representation of individual fits to the ^{98}Mo(2^+_1) data at (a) 13.2 MeV and (b) 16.0 MeV.

variation of the parameters C_2 and δ_2^N contemplates this discrepancy, which probably contains physical information outside the proposed reaction model. This fact is illustrated through Fig. 7, which presents the constant χ^2 contour lines [6] corresponding to alternative individual (unconstrained) best fits to each, the angular distribution at 13.2 MeV and that at 16.0 MeV, for ^{98}Mo, where both C_2 and δ_2^N were allowed to vary, at each energy. The contour lines are approximately elliptical and, at 13.2 MeV, centered at about the same values of C_2 and δ_2^N, as formerly obtained in the constrained analysis. On the other hand, the results of an unconstrained analysis at 16.0 MeV show, as could be expected, C_2 to be rather poorly defined at this energy. Furthermore, since the value of C_2 affects δ_2^N in a covariant manner, this last value also wanders outside the regions defined by the better data at 13.2 MeV. It is, however, to be remembered that when comparison between the values of δ_2^N, extracted at both incident energies, is to be done, the scale uncertainties in the cross sections have to be included. The sum of the minimum χ^2 values obtained in the individual fits performed at the two energies, which equals 124.0, is only somewhat lower than that resulting from the constrained analysis and, even with the opportunity of varying the parameters freely, no fit to the discrepancy at the first maximum of either of the angular distributions was achieved.

B. Octupolar excitations

Due to their much reduced Coulomb excitation probability, the transition to the 3^-_1 states is strongly dominated by the nuclear interaction. Nevertheless, as Fig. 8 reveals, at 13.2 MeV enough structure change remains at the forward angles of the predicted angular distribution to obtain some information on C_3. In Fig. 8 the separate contributions of the Coulomb and nuclear interactions to the excitation of the octupolar states are represented, respectively, as dotted and dashed lines, at both deuteron energies. For comparison, similar information is also presented for the quadrupolar excitations. In all instances, the most prominent change resulting from the inclusion of the Coulomb excitation is the development of an interference minimum at forward angles.

Constrained (same C_3) analyses of the first octupolar excitations in ^{94,98}Mo at 13.2 and 16.0 MeV incident deuteron energy were performed employing the same statistical analysis as for the quadrupolar ones. The results are shown in Fig. 9, again for increased radii (solid lines) and for the original global parameters (dashed lines). Data for the 3^-_1 excitations are affected, for a considerable range of detection angles, $\theta_{\rm lab} \geqslant 60°$, by the unavoidable presence of contaminant elastic peaks associated with carbon and oxygen (see Fig. 1).

The contour lines for constant χ^2, associated with the alternative unconstrained best fits at 13.2 MeV and at 16.0 MeV, are presented in Fig. 10, for the octupolar excitation in ^{94}Mo. It is clear that the data at 16.0 MeV are almost useless to define C_3. Since the contour lines are not ellipses, being, in fact, rather asymmetric with respect to $\chi^2_{\rm min}$, it is possible

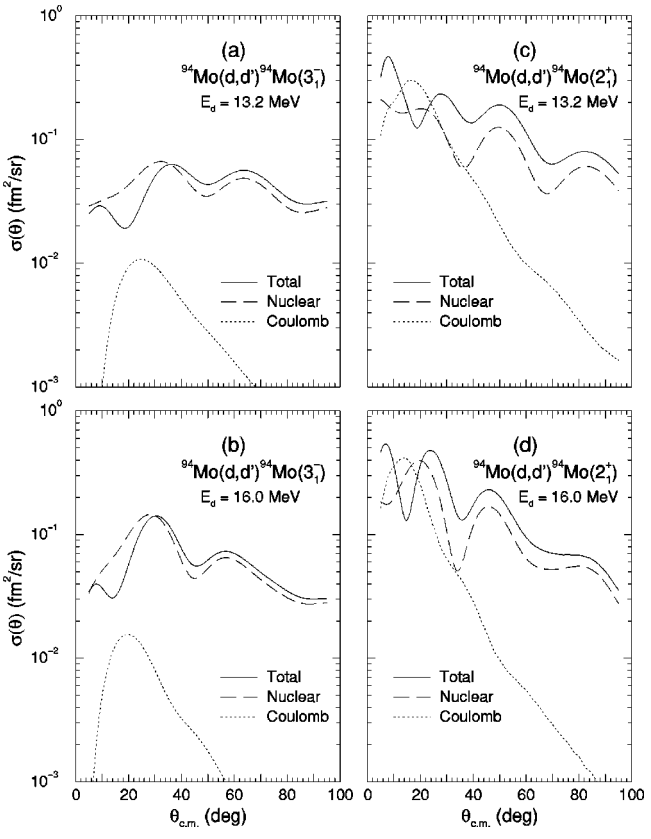

FIG. 8. The influence of Coulomb excitation on DWBA-DOMP predictions for the angular distributions in the excitation of, respectively, the 3^-_1 state [(a) and (b)] and the 2^+_1 state [(c) and (d)], for both deuteron energies employed. The values for ^{94}Mo are taken as an example, but no essential difference is verified for ^{98}Mo.

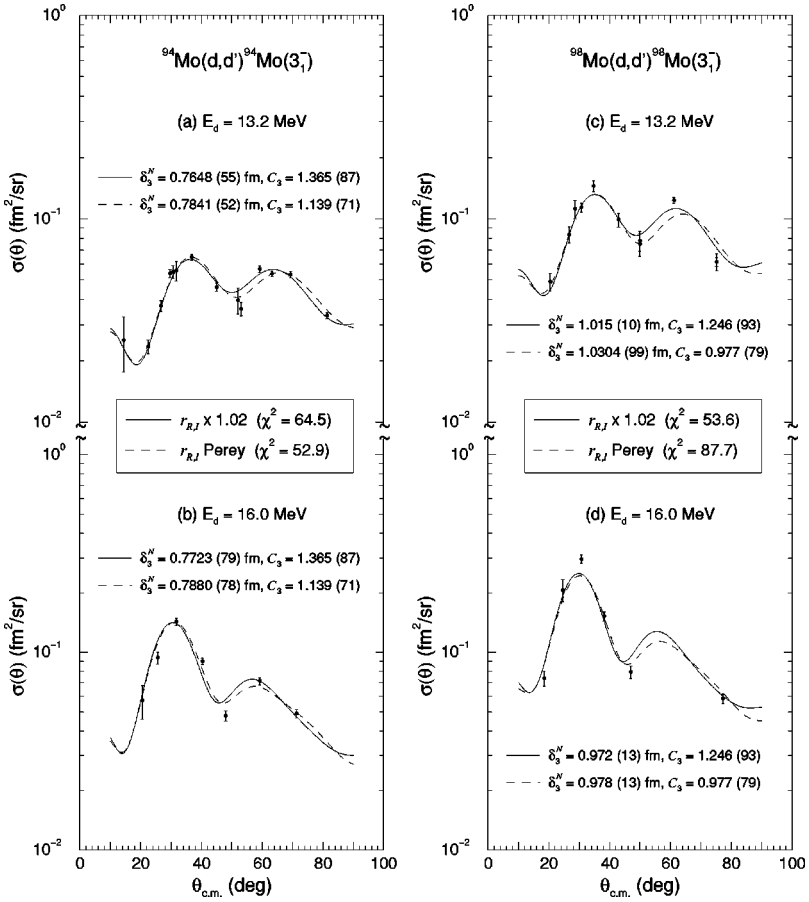

FIG. 9. Experimental angular distributions for the octupolar excitations in ^{94}Mo and ^{98}Mo, at two incident deuteron energies, in comparison with DWBA-DOMP best fits, for which the same value of C_3 was imposed. Solid lines correspond to the predictions for increased radii (+2%), while broken lines correspond to the predictions with the original Perey-Perey parameters. The χ^2 values characterize the quality of the constrained simultaneous fit to both angular distributions, for each isotope.

that C_3 is affected [6] by somewhat greater uncertainties than stated. Even so, as indicated in Fig. 9, the values obtained in the constrained analysis for the parameters δ_3^N and C_3, with and without the 2% increase in the radii, are almost compatible within the attributed uncertainties.

IV. DISCUSSION AND CONCLUSIONS

The results of the present experiment for the quadrupolar and octupolar excitations in ^{94,98}Mo, obtained within the adopted analysis (DWBA-DOMP with global optical parameters) are compiled in Table III. The values presented for δ_L^N are, for both isotopes, a weighted mean of the two informations, at 13.2 and 16.0 MeV, including the scale uncertainty in the cross sections of, respectively, $\pm 5\%$ and $\pm 7\%$. The ratios $B(EL)/B(ISL)$ are also presented in Table III. Values of $r_C = 1.22$ fm and $r_m = 1.16$ fm were employed for the reduced radii of the equivalent sharp cutoff uniform charge and, respectively, mass distributions [6]. An uncertainty of $\pm 5\%$ was associated with r_m in the ratios $B(EL)/B(ISL)$. The values extracted for M_n/M_p, in comparison with the values of N/Z, expected for a homogeneous collective excitation of the mass distributions, are also shown. It is, however, to be stressed, that the ratios M_n/M_p are affected, not only by rather important propagated experimental uncertainties [verify expression (7)], but also by uncertainties due to the underlying theoretical hypotheses, which are difficult to specify, but should preserve at least one significant figure.

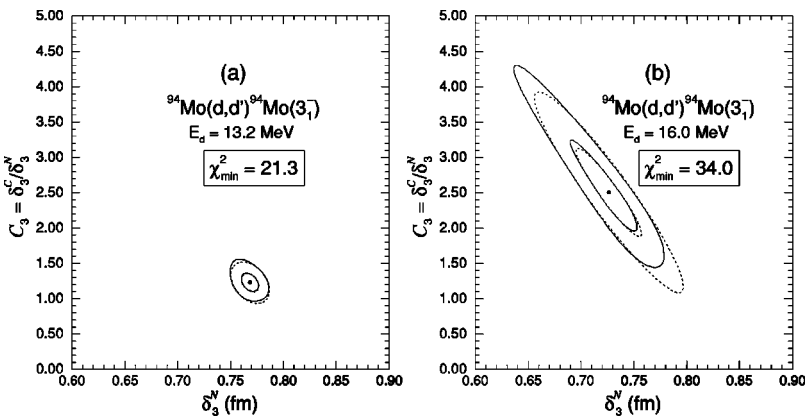

FIG. 10. Comparison of the contour lines for constant χ^2 (solid lines) with the ellipses that result from the Gauss-Marquardt method (broken lines) for intervals corresponding to, respectively, 68.3% ($\Delta\chi^2 = 2.3$) and 99.7% ($\Delta\chi^2 = 11.8$) of statistical confidence, in the representation of individual fits to the ^{94}Mo(3_1^-) data at (a) 13.2 MeV and (b) 16.0 MeV.

TABLE III. Parameters C_L and δ_L^N extracted in the present paper. Also indicated are the values of the ratios $B(EL)/B(ISL)$, M_n/M_p, and N/Z.

A	State	C_L	$\overline{\delta_L^N}$ (fm)	$\overline{\beta_L^N}$ [a]	$B(EL)/B(ISL)$ (e^2)	M_n/M_p	N/Z
94	2_1^+	1.123(20)	0.792 (17)	0.152 (3)	1.39(15)	0.89	1.24
98	2_1^+	1.148(24)	0.883 (19)	0.167 (4)	1.46(16)	0.93	1.33
94	3_1^-	1.14 (7)	0.785 (17)	0.150 (3)	1.6 (4)	0.8	1.24
98	3_1^-	0.98 (8)	1.011 (22)	0.191 (4)	1.2 (3)	1.2	1.33

[a] $\overline{\beta_L^N} = \overline{\delta_L^N}/1.15A^{1/3}$.

The uncertainties extracted through the statistical method of analysis employed [6], reflect (through a factor of about 4) the lower sensitivity of the data to the ratio C_3, in comparison with what is verified for C_2, while the deformation length δ_3^N is approximately as well determined as δ_2^N. The deformation parameters β_L^N calculated from the experimental mean values of δ_L^N, agree with β_L values formerly obtained in proton inelastic scattering [15,16] and in the 21.5 MeV deuteron inelastic experiment [17], both of which are influenced predominantly by the nuclear excitation. Incidentally, the experimental angular distributions of these older studies also indicate that a small increase in the radii of the optical potentials could provide a better fit to the inelastic results.

The values of $C_2 > 1.0$ and $C_3 \geqslant 1.0$, extracted in the present CNI studies for ^{94}Mo and ^{98}Mo, indicate that the protons contribute more than the neutrons to both the 2_1^+ and the 3_1^- excitations. The values $M_n/M_p \sim 0.9$ obtained for the quadrupolar excitations in ^{94}Mo and ^{98}Mo, being smaller than the $N/Z = 1.2$–1.3 expected from the homogeneous collective model, are another way to characterize the role played by the protons relative to the neutrons in these excitations.

The values $C_2 = 1.123(20)$ and $C_2 = 1.148(24)$ are about the same for ^{94}Mo and ^{98}Mo and, as a consequence, so are also the ratios $B(E2)/B(IS2)$. In a previous CNI study of inelastic scattering of alpha particles on ^{100,102,104}Ru [8], values of C_2 increasing from 1.04 to 1.22, had been found for that isotopic chain, demonstrating, also for Ru, a slight predominance of the protons. On the contrary, neutrons contribute more than protons to the first quadrupolar excitations in the isotones ^{92}Zr and ^{96}Zr. Values of M_n/M_p close to 2, for ^{92}Zr [7,18,19], and to 4, for ^{96}Zr [7,19], were reported in inelastic-scattering studies with alpha particles and ^{6}Li.

The evolution of the $B(ISL)$ and $B(EL)$ values between ^{94}Mo and ^{98}Mo, considering also the $B(EL)$ values adopted in the literature [1,20], may be examined through the ratios given in Table IV. These show the 2_1^+ excitation to be somewhat more collective in ^{98}Mo than in ^{94}Mo, for both mass and charge contributions. The parallel evolution of the $B(ISL)$ and the $B(EL)$ from ^{94}Mo to ^{98}Mo (compare values in columns 2 and 3 of Table IV, and note their compatibility) for the first collective 2^+ states, shows again that the isospin characteristics of these excitations do not change drastically, in contrast to what happens in the Zr isotopes. The agreement of the relative values of the $B(E2)$ with those resulting from the adopted ones [1] is good, although the absolute values determined in the present paper are higher, for both ^{94,98}Mo. It is to be noted that for $B(E2)$ the adopted values [1] are heavily based on the results of one laboratory; furthermore, for ^{94}Mo, there are several experimental results, spread over a considerable range. The octupolar excitation is also more collective in ^{98}Mo than in ^{94}Mo, the agreement with published $B(E3)$ values occuring within 2 standard deviations.

Summarizing, inelastic scattering of deuterons is presented as a convenient means of conveying information on the isospin character of collective excitations of low multipolarity, especially of the important 2_1^+ state, in the mass region of $A \sim 100$. For this purpose, the parameter $C_2 = \delta_2^C/\delta_2^N$ is defined (where the $\delta_2^{C,N}$ are the quadrupolar deformation lengths corresponding, respectively, to the charge and the mass excitations), as a measure of the relative contribution of protons (charge) and of protons plus neutrons (mass). The value of $C_2 = 1.0$ corresponds to the expectation of a homogeneous collective model. It is felt [6] that, when considering CNI results with a macroscopic description, C_2 is a better representation for any predominance of protons or neutrons in a particular 2_1^+ excitation than, for instance, M_n/M_p or either $B(E2)$ or $B(IS2)$ separately, since in the extraction of the C_L parameter, several systematic uncertainties of experimental and/or theoretical nature are cancelled. The values of C_2 may be directly translated into ratios of $B(E2)/B(IS2)$ and/or M_n/M_p, but the first ones are, additionally, affected by choices of reduced charge and mass

TABLE IV. Evolution of $B(ISL)$ and $B(EL)$ values between ^{94}Mo and ^{98}Mo.

	Present work		Literature
State	$B(ISL)_{(98)}/B(ISL)_{(94)}$	$B(EL)_{(98)}/B(EL)_{(94)}$	$B(EL)_{(98)}/B(EL)_{(94)}$
2_1^+	1.28 (8)	1.34 (8)	1.32(4)[a]
3_1^-	1.75(11)	1.29(26)	2.2 (5)[b]

[a] Reference [1].
[b] Reference [20].

radii, while in the extraction of the latter, further theoretical hypotheses are made.

The values of C_2 obtained in the present work reveal the 2_1^+ excitations in ^{94}Mo and ^{98}Mo to be not homogeneous, but with only a slight predominance of the protons. This is in marked contrast with what was observed for the isotones ^{92,96}Zr where neutrons strongly dominate the transitions [7,18,19]. For the other isotone of ^{98}Mo, ^{100}Ru, the first quadrupolar excitation had been previously characterized as almost homogeneous [8]. The quadrupolar excitation in ^{98}Mo is somewhat more collective than the corresponding one in ^{94}Mo, so no depression of collectivity due to a $N=56$ subshell closure is apparent for ^{98}Mo. In fact, the excitation energies of the 2_1^+ states in the sequence $^{94-98}$Mo are, accordingly, decreasing.

ACKNOWLEDGMENTS

Financial support by CAPES (Coordenação de Aperfeiçoamento de Pessoal de Nível Superior), CNPq (Conselho Nacional de Desenvolvimento Científico e Tecnológico), FINEP (Financiadora de Estudos e Projetos), and FAPESP (Fundação de Amparo à Pesquisa do Estado de São Paulo) is gratefully acknowledged.

[1] S. Raman, C. H. Malarkey, W. T. Milner, C. W. Nestor, and P. H. Stelson, At. Data Nucl. Data Tables **36**, 1 (1987).
[2] T. R. Werner, J. Dobaczewski, M. W. Guidry, W. Nazarewicz, and J. A. Sheikh, Nucl. Phys. **A578**, 1 (1994).
[3] J. Skalski, S. Mizutori, and W. Nazarewicz, Nucl. Phys. **A617**, 282 (1997).
[4] S. Åberg, H. Flocard, and W. Nazarewicz, Annu. Rev. Nucl. Part. Sci. **40**, 439 (1990).
[5] J. L. M. Duarte, T. Borello-Lewin, G. Maino, and L. Zuffi, Phys. Rev. C **57**, 1539 (1998).
[6] J. L. M. Duarte, G. M. Ukita, T. Borello-Lewin, L. B. Horodynski-Matsushigue, and L. C. Gomes, Phys. Rev. C **56**, 1855 (1997).
[7] D. Rychel, R. Gyufko, B. van Kruchten, M. Lahanas, P. Singh, and C. A. Wiedner, Z. Phys. A **326**, 455 (1987).
[8] L. C. Gomes, L. B. Horodynski-Matsushigue, T. Borello-Lewin, J. L. M. Duarte, J. H. Hirata, S. Salém-Vasconcelos, and O. Dietzsch, Phys. Rev. C **54**, 2296 (1996).
[9] D. Pulino, G. M. Sipahi, G. M. Ukita, T. Borello-Lewin, L. B. Horodynski-Matsushigue, J. L. M. Duarte, W. G. P. Engel, and J. C. de Abreu, Rev. Bras. Aplicações Vácuo **10**, 87 (1991).
[10] C. M. Perey and F. G. Perey, At. Data Nucl. Data Tables **17**, 1 (1976).
[11] W. W. Daehnick, J. D. Childs, and Z. Vrcelj, Phys. Rev. C **21**, 2253 (1980).
[12] G. R. Satchler, *Direct Nuclear Reactions* (Clarendon, Oxford, 1983).
[13] P. D. Kunz, computer code DWUCK4 version, Colorado University, 1974 (private communication).
[14] D. J. Horen *et al.*, Phys. Rev. C **44**, 128 (1991).
[15] H. F. Lutz, D. W. Heikkinen, and W. Bartolini, Phys. Rev. C **4**, 934 (1971).
[16] Y. Awaya, K. Matsuda, T. Wada, N. Nakanishi, S. Takeda, and S. Yamaji, J. Phys. Soc. Jpn. **33**, 881 (1972).
[17] T. Wada, Nucl. Phys. **A307**, 425 (1978).
[18] L. B. Horodynski-Matsushigue, T. Borello-Lewin, and J. L. M. Duarte, Proceedings of the International Nuclear Physics Conference, Universidade de São Paulo, Brazil, 1989 (unpublished), Vol. I, p. 307.
[19] D. J. Horen, G. R. Satchler, S. A. Fayans, and E. L. Trykov, Nucl. Phys. **A600**, 193 (1996).
[20] R. H. Spear, At. Data Nucl. Data Tables **42**, 55 (1989).